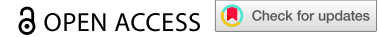Taylor & Francis
Taylor & Francis Group

BRIEF REPORT

Preclinical characterization of an mRNA-encoded anti-Claudin 18.2 antibody

Hayat Bähr-Mahmud[a]*, Ursula Ellinghaus[a]*, Christiane R. Stadler[a], Leyla Fischer[a], Claudia Lindemann [a], Anuhar Chaturvedi [a], Jan Diekmann[a], Stefan Wöll[a], Imke Biermann[a], Bernhard Hebich[a], Caroline Scharf[a], Manuela Siefke[a], Alexandra S. Roth[a], Martin Rao [a], Kerstin Brettschneider[a], Eva-Maria Ewen[a], Uğur Şahin [a,b], and Özlem Türeci[a,c]

[a]BioNTech SE, Mainz, Germany; [b]TRON gGmbH–Translational Oncology at the University Medical Center of the Johannes Gutenberg University, Mainz, Germany; [c]HI-TRON (Helmholtz Institute for Translational Oncology) Mainz by DKFZ, Mainz, Germany

ABSTRACT

IMAB362/Zolbetuximab, a first-in-class IgG1 antibody directed against the cancer-associated gastric-lineage marker CLDN18.2, has recently been reported to have met its primary endpoint in two phase 3 trials as a first-line treatment in combination with standard of care chemotherapy in CLDN18.2-positive Her2 negative advanced gastric cancer. Here we characterize the preclinical pharmacology of BNT141, a nucleoside-modified RNA therapeutic encoding the sequence of IMAB362/Zolbetuximab, formulated in lipid nanoparticles (LNP) for liver uptake. We show that the mRNA-encoded antibody displays a stable pharmacokinetic profile in preclinical animal models, mediates CLDN18.2-restricted cytotoxicity comparable to IMAB362 recombinant protein and inhibits human tumor xenograft growth in immunocompromised mice. BNT141 administration did not perpetrate mortality, clinical signs of toxicity, or gastric pathology in animal studies. A phase 1/2 clinical trial with BNT141 mRNA-LNP has been initiated in advanced CLDN18.2-expressing solid cancers (NCT04683939).

Introduction

Based on systematic *in silico* cancer target discovery screening, we proposed splice variant 2 of the tight-junction protein claudin 18 (CLDN18.2) as an ideal tumor-associated target for monoclonal antibody therapy of various cancer types.[1] CLND18.2 is a highly selective gastric-lineage marker expressed exclusively in differentiated cells of gastric epithelia, but not in any other normal human cell type.[2] In normal gastric tissue, CLDN18.2 is buried in the tight-junction supramolecular complex of stomach lining cells. Loss of cell polarity and disruption of the tight-junction architecture during malignant transformation exposes CLDN18.2 epitopes on gastric tumor cells, rendering these cells targetable by intravenously administered CLDN18.2-directed antibodies. In addition to its lineage-related expression in gastric cancers, CLDN18.2 is aberrantly activated in various other cancers, such as esophageal,[1,3] pancreatic[4] (including precancerous lesions),[5,6] mucinous ovarian,[1] biliary,[7] and lung cancers.[8]

We previously reported development of IMAB362 (INN: Zolbetuximab), a first-in-class, chimeric monoclonal IgG1 antibody that binds to CLDN18.2 with high selectivity and mediates tumor cell death through antibody-dependent cellular cytotoxicity (ADCC) and complement-dependent cytotoxicity (CDC), which are Fcγ receptor-dependent mechanisms.[9]

IMAB362 has shown single-agent activity and a manageable safety profile in studies involving patients with heavily pretreated recurrent or refractory CLDN18.2-positive gastric and gastroesophageal junction (G/GEJ) cancer.[10–12] In a randomized phase 2 trial in patients with newly diagnosed advanced CLDN18.2-positive gastroesophageal adenocarcinoma, we showed that IMAB362 as an add-on to first-line EOX (epirubicin, oxaliplatin, and capecitabine) chemotherapy provides a statistically significant benefit over EOX alone on progression-free survival, overall survival, objective response rate[13] and improved quality of life.[14] Recently, two randomized phase 3 trials testing IMAB362 in combination with standard-of-care chemotherapy regimens in patients with G/GEJ showed improved progression-free and overall survival as compared to chemotherapy alone.[15,16]

In our pursuit to develop next-generation modalities targeting CLDN18.2, we are exploring RNA therapeutics encoding antibodies that we call RiboMabs.[17] RiboMabs are RNA-encoded antibody sequences packaged in lipid nanoparticles (LNPs) that are administered intravenously, taken up and translated to the encoded antibody in the liver. We have previously reported for RNA-LNPs encoding a bispecific T cell-engaging antibody that their repeated delivery results in sustained production of therapeutic levels of that bispecific antibody in mice.[17] The present study describes the preclinical pharmacology and anti-tumor activity of BNT141, an LNP-encapsulated N1-methylpseudouridine-modified RNA therapeutic encoding for an antibody sequence identical to IMAB362, referred

to here as RiboMab01 to distinguish the BNT141-derived antibody from recombinantly produced IMAB362. The data presented here has informed the design of the first-in-human phase 1 trial with BNT141 as monotherapy and in combination with chemotherapy in patients with CLDN18.2-expressing gastric, pancreatic, ovarian, and biliary tract tumors refractory to standard-of-care treatment (NCT04683939).

Materials and methods

Animals

Female BALB/cJRj mice (Janvier Labs) were purchased at 7 to 8 weeks of age and 24 g average body weight. Female immuno-deficient Hsd:Athymic Nude-Foxn1nu/nu (Envigo) mice were purchased at 11 weeks of age and 25 g average body weight. All mouse studies were approved by the regional animal welfare committee (ethical approval no. 23 177–07/G 17-12-001), conducted per Federation of Laboratory Animal Science Association (FELASA) recommendations and in compliance with the German Animal Welfare Act and EU Directive 2010/63/EU. Recommendations of the *Gesellschaft für Versuchstierkunde*/Society of Laboratory Animal Science (GV-SOLAS) were additionally applied. The nonhuman primate (NHP) study was conducted at the Laboratory of Pharmacology and Toxicology GmbH & Co. KG (Hamburg, Germany). Female cynomolgus monkeys (Roberto C. Hartelust, Tilburg, the Netherlands) were 3 to 4 years old and weighed 2.5 to 3.4 kg at the initiation of dosing. The monkeys were housed in V2A steel cages in collectives of up to three animals with only one treatment group per collective at room temperature of 23 ± 3°C (maximum range) and the relative humidity at 60 ± 20% (maximum range). Rooms were alternately lit and darkened in a 12-h cycle. Animals were fed with commercial diet ssniff® Pri V3994 (ssniff Spezialdiäten GmbH, 59494 Soest, Germany). Drinking water was offered *ad libitum*.

Cells and cell culture

The following cell lines were used in this study: Chinese hamster ovary (CHO) K1 cells (ATCC CCL-61); luciferase (Luc)-expressing CHO-K1 cell lines with and without a stable human CLDN18.2 transgene; human gastric adenocarcinoma cell lines NCI-N87 (ATCC CRL-5822) and NUGC-4 (JCRB0834; 46% cells constitutively CLDN18.2+) engineered to overexpress human CLDN18.2 (NUGC-4~hCLDN18.2; 94% cells CLDN18.2+) and harboring a Luc transgene; transfected CLDN18.2-overexpressing NCI-N87 without a Luc transgene (NCI-N87~hCLDN18.2; 60% cells CLDN18.2+); MDA-MB-231 human breast adenocarcinoma cells (ATCC HTA-26) with and without Luc expression. All cell lines were cultured per standard procedures recommended by the provider.

Primary human hepatocytes used for lipofections were cultured according to the manufacturer's instructions (BioIVT). Peripheral blood mononuclear cells (PBMC) were isolated by Ficoll density-gradient centrifugation from buffy coats of healthy human donors (Mainz University Hospital) for use as ADCC effectors.

Cloning, in vitro transcription of RNA and LNP encapsulation

RiboMab01-encoding DNA sequences were human codon-optimized prior to gene synthesis. The anti-CLDN18.2 domain heavy and light chain sequences were derived from the previously published IMAB362 full-length IgG antibody sequence.[18] *Spe*I-*Xho*I restriction sites were added to the DNA sequences; digestion with *Spe*I and *Xho*I yielded fragments of 1,474/3,974 and 790/3,974 base pairs for the heavy and light chain DNA constructs, respectively, which were sequenced and compared with the IMAB362 sequence. In addition to the heavy and light chain-encoding sequences, each transcribed RNA strand contains common structural elements optimized for stability and translational efficiency (CC413 as 5'-cap, AGA-dEarI-hAg as 5'-untranslated region [UTR], FI element as 3'-UTR, and a poly[A] tail measuring 100 adenosines with a linker at position 30 [A30L70]).[19,20]

In vitro transcription of the RiboMab01-encoding heavy chain and light chain DNA sequences was performed as previously described.[17] The resulting 5', N1-methylpseudouridine (m1Ψ)-capped RNA was isolated with magnetic beads, purified with cellulose, diluted in RNAse-free water (B. Braun) and stored in nuclease-free reaction tubes (Eppendorf). The transcribed RNA was quality-assessed (Agilent 2100 Bioanalyzer, Agilent Technologies Inc.) and quantitated (Nanodrop 2000c, Thermo Fisher Scientific) prior to encapsulation in LNP (ionizable cationic lipid, a polyethylene glycol (PEG) lipid, phospholipid, and cholesterol) to generate BNT141, followed by storage at −65 to −85°C. The formulations were tested for particle size, distribution, encapsulation efficiency, and RNA concentration. Typically, the LNP sizes were approximately 70 nm, polydispersity index < 0.1, encapsulation efficiency >90% and RNA concentration ~1 mg/mL. RNA-LNP doses or concentrations are given as masses or concentrations of encapsulated-RNA.

Lipofection of cells

Primary human hepatocytes were thawed per the provider's instructions (BioIVT), resuspended in InVitroGro™ CP medium (Merck KGaA) + Torpedo™ Antibiotic Mix (BioIVT) and seeded at 2.5×10^4 cells/well on a BioCoat™ Collagen I 96-well plate (Corning). After allowing 2 to 4 h for cell adhesion, the medium was replenished and the plate incubated for a further 24 h. The culture medium was then exchanged for InVitroGro HI medium + antibiotics. BNT141 serial dilution in saline was added and the plate incubated for 48 h at 37°C, 5% CO_2. After centrifugation (300 ×g, 4 min), the resulting supernatant was pooled and stored at 2 to 8°C until analysis.

CHO-K1 cells suspended in F-12K Nutrient mixture medium (Thermo Fisher Scientific) + 10% fetal bovine serum (FBS) were seeded at 1×10^5 cells/well on a 48-well plate 24 h before lipofection. Culture medium was exchanged for Opti-MEM® I Reduced Serum Medium (Thermo Fisher Scientific) followed by addition of serially diluted BNT141 to the test wells, PBS or

erythropoietin (EPO)-encoding RNA-LNP to the control wells and a 48-h incubation at 37°C, 5% CO_2. The cell culture supernatant was harvested by centrifugation (500 ×g, 10 min), transferred to a clean 96-well plate, pooled, and stored at 2 to 8°C until analysis.

Pharmacokinetic studies

Ten-to-fourteen-week-old female BALB/cJRj mice received an IV bolus of BNT141 (1, 3, 10, or 30 µg; $n = 3$/group) to determine RiboMab01 pharmacokinetics (PK) after single and repeated (five weekly injections) dosing. Negative control mice received 30 µg Luc RNA-LNP ($n = 3$), while animals in the reference group ($n = 3$) were given IMAB362 (40 µg [single dose] or 80 µg [repeated-dose]). For plasma preparation, peripheral blood was collected in Microvette 300 LH tubes at earlier time points or Microvette 500 Z-Gel at later time points (both from Sarstedt) and centrifuged (10,000 × g, 5 min) at room temperature. Plasma was aliquoted and stored frozen (−65 to −85°C) until analysis.

Three-to-four-year-old female cynomolgus monkeys were given three weekly IV boluses of 0.1, 0.4, or 1.6 mg/kg BNT141 ($n = 3$/group), saline ($n = 3$) or empty LNP ($n = 3$). Serum was prepared from venous blood at various time points, aliquoted, and stored at −20 ± 2°C until analysis.

Sandwich enzyme-linked immunosorbent assay (ELISA) for RiboMab01 quantitation

The ELISA assays were performed with kits, a measuring device and analysis software from Gyros Protein Technologies AB. Serum or plasma samples were first diluted 10-fold and cell culture supernatant samples twofold. RiboMab01 in serum/plasma was captured using a biotinylated anti-human IgG Fc antibody and detected with an Alexa Fluor® 647-labeled anti-human IgG (Gyrolab Generic PK/TK Kit – Low/High-Titer). In cell culture supernatant, a biotinylated derivative of *Staphylococcus aureus* protein A was used for capture and an Alexa Fluor® 647-labeled F(ab´)$_2$ fragment of anti-human IgG (Gyrolab huIgG Kit – Low Titer) for detection. Low-titer PK analysis was performed in a Gyrolab Bioaffy 1000 HC CD with dynamic ranges of 0.5 to 1,000 ng/mL in serum/plasma and 4 to 3,000 ng/mL in cell culture supernatant. High-titer PK analysis was performed in a Gyrolab Bioaffy 20 HC CD with a 0.05 to 200 µg/mL dynamic range in serum/plasma. IMAB362 served as reference.

Cytotoxicity assays

ADCC: 3×10^5 human PBMC were added to 1×10^4 luciferase-expressing NUGC-4~hCLDN18.2 target cells or MDA-MB-231 control cells in assay medium (RPMI 1640 medium + 10% FBS +100 U/mL penicillin +100 U/mL streptomycin +1 M HEPES; Thermo Fisher Scientific) on a white 96-well microtiter plate. Serially diluted RiboMab01-containing CHO-K1 supernatant, plasma or sera from BNT141-dosed animals was added to the experimental lysis wells (L_{exp}) in triplicate. IMAB362 was used as reference. Mock (buffer only)-lipofected CHO-K1 cell culture supernatant was used as

sample diluent and added to the minimum and maximum lysis (L_{min}, L_{max}) wells. Plates were incubated at 37°C, 5% CO_2 for 48 h.

CDC: 2.5×10^4 luciferase-expressing target and control cells prepared in medium A (DMEM/F-12 medium + 10% FBS +20 mM HEPES; Thermo Fisher Scientific) were seeded on a white 96-well microtiter plate in triplicate and incubated at 37°C, 5% CO_2 for 24 h. Culture supernatant from BNT141-lipofected CHO-K1 cells, sera from BNT141-dosed animals or IMAB362 reference antibody were serially diluted and added to the test (L_{exp}) wells. The L_{min} wells contained only mock culture supernatant + FBS-free medium A (diluent). A final concentration of 25% non-heat-inactivated normal human serum (Quidel) as complement source was added per well and incubated at 37°C, 5% CO_2 for 140 min.

ADCC and CDC: the L_{max} wells were treated with 20% Triton X-100 for 10 min and the assay plates incubated with buffered BD Monolight luciferin (BD Biosciences) for 30 min. Bioluminescence was measured on an Infinite M200 microplate reader (Tecan) and the percentage of specific target cell lysis calculated as follows:

$$\text{Specific lysis}(\%) = \left\{1 - [L_{exp} - L_{max}]/[L_{min} - L_{max}]\right\}\text{x}10$$

Human tumor xenograft mouse model

Eleven-week-old female Hsd:Athymic Nude-Foxn1 nu/nu mice were subcutaneously injected with 5×10^6 NCI-N87 ~hCLDN18.2 cells in the upper right flank. Body weight was recorded at the start and weekly throughout the study. The largest (a) and smallest (b) tumor diameters were measured with a caliper every 2 to 4 days to calculate the tumor volume:

$$\text{Tumor volume } = \left\{a[mm] \text{ x } b[mm]_2\right\}/ 2$$

Upon reaching a mean tumor volume of 30 mm^3, the animals were randomly distributed to six groups of nine mice each: 3, 10 or 30 µg BNT141 (test groups), 30 µg Luc RNA-LNP (negative control), 800 µg IMAB362 (reference) or saline (vehicle). A total of six injections were administered weekly by IV bolus.

The mean tumor volume per group at the end of the study (day 56) was normalized to the Luc RNA-LNP group to calculate the relative tumor volume percentages:

$$\begin{aligned}&\text{relative tumor volume}(\%)\\ &= 100 - \left\{[\text{Mean}_{\text{treatment group}}/\text{Mean}_{\text{Luc RNA} - \text{LNP}}] * 100\right\}\end{aligned}$$

Data analysis and statistics

Graphs were produced and analyzed using GraphPad Prism 9 software. The Mann–Whitney U test was applied to compare groups. The sigmoidal dose–response (standard slope) algorithm was used to visualize and analyze ADCC and CDC data.
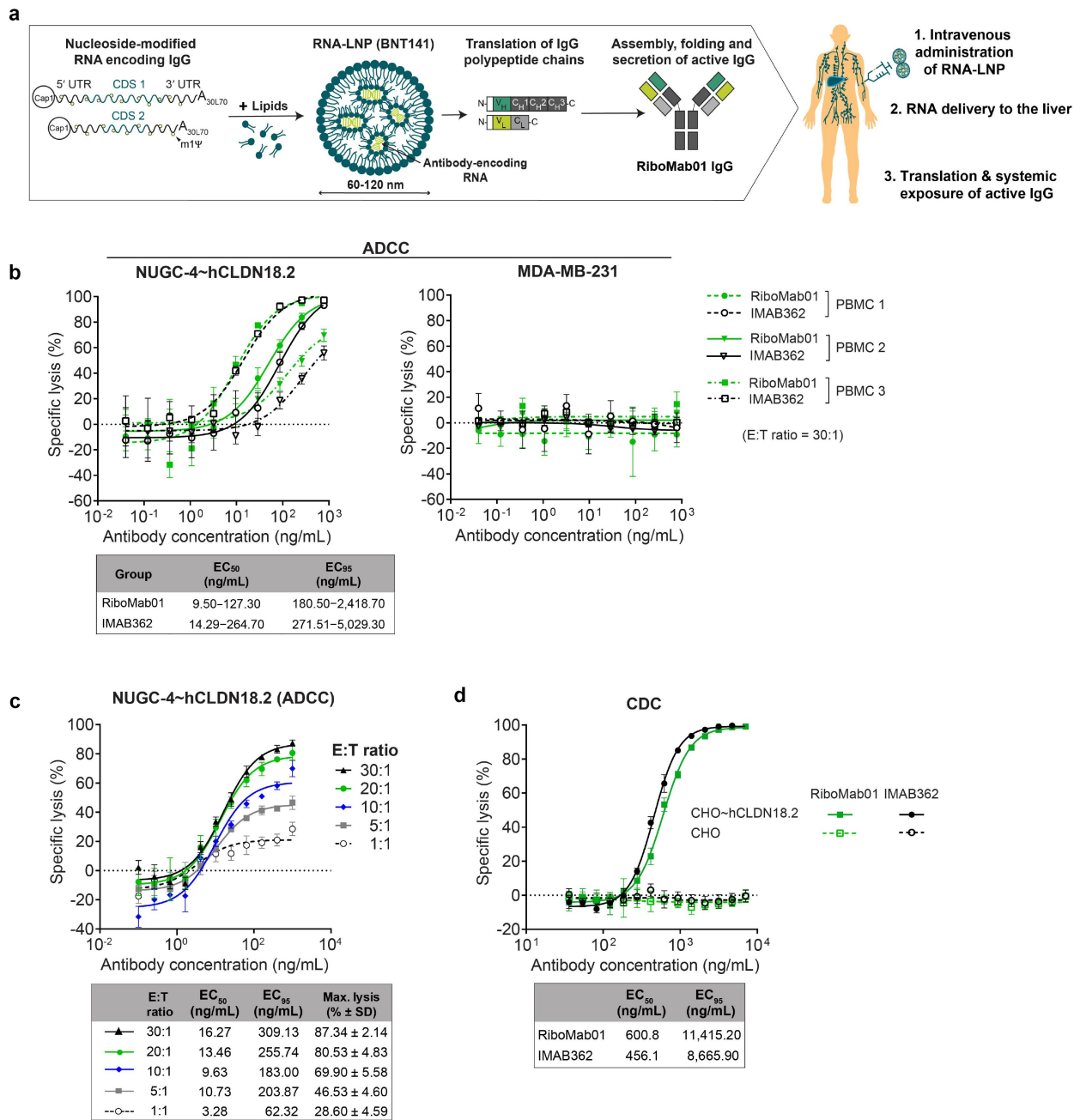
Figure 1. BNT141-encoded RiboMab01 produced *in vitro* is biologically active. (a) Schematic representation of the RiboMab® platform and its anticipated mode of action *in vivo*. (b) RiboMab01-mediated ADCC after 48 h of co-incubation of human PBMC (*n* = 3) with NUGC-4~hCLDN18.2 gastric adenocarcinoma cells or CLDN18.2-negative MDA-MB-231 breast adenocarcinoma cells at a 30:1 E:T ratio. (c) RiboMab01-mediated ADCC after 24 h of co-incubation of human PBMC with NUGC-4~hCLDN18.2 cells at different E:T ratios. (d) RiboMab01-mediated CDC after 4 h of co-incubation of CHO-K1~hCLDN18.2 or CLDN18.2-negative CHO-K1 with 25% human serum as complement source. ADCC and CDC assays were conducted with RiboMab01-containing supernatant from BNT141-lipofected CHO-K1 cells; IMAB362 was used as a reference antibody. Data are means ± SD of technical triplicates. ADCC, antibody-dependent cellular cytotoxicity; CDC, complement-dependent cytotoxicity; CHO, Chinese hamster ovary; E:T, effector-to-target; PBMC, peripheral blood mononuclear cells.

Results

BNT141-encoded RiboMab01 produced *in vitro* is biologically active

BNT141 RNA-LNPs consist of two single-stranded RNAs encoding the light and the heavy chain of the CLDN18.2-specific IgG1 IMAB362/Zolbetuximab (Figure 1a). We selected this monoclonal antibody clone for its selective binding to its target CLDN18.2, as confirmed by a tissue cross-reactivity study that did not detect unspecific cross-reactivity to any healthy human tissues except for the gastric mucosa epithelium (Figure S1).

First, we assessed whether expression of BNT141 in eukaryotic cells yields an antibody with the same functionality as IMB362. Primary human hepatocytes and CHO-K1 cells transfected with BNT141 secrete RiboMab01 as a correctly assembled, structurally stable monomeric IgG molecule. RiboMab01 produced *in vitro* bound human CLDN18.2-overexpressing gastric adenocarcinoma cell lines (Figure S2). RiboMab01 mediated dose-dependent, potent

CLDN18.2-specific ADCC with EC_{50} values ranging between 9 and 127 ng/mL reaching maximum lysis of 70 to 98% (Figure 1b). Cytolysis of CLDN18.2-expressing tumor cells by RiboMab01 was optimal at an effector-to-target (E:T) ratio of 30:1, with robust killing observed at E:T ratios as low as 5:1 (Figure 1c). RiboMab01 also exhibited potent CLDN18. 2-specific CDC of stably CLDN18.2-expressing CHO cells with an EC_{50} value of 600 ng/ml and 100% maximum killing (Figure 1d). RiboMab01 and IMAB362 mediated ADCC and CDC with similar efficacies (Figure 1b, d).

BNT141 exerts anti-tumor activity in a human tumor xenograft mouse model

To assess whether IV-administered BNT141 RNA-LNP results in bioavailable and functional antibody *in vivo* with the capacity to mediate anti-tumor activity, we resorted to studies in nude mice bearing a subcutaneous CLDN18.2-expressing human gastric tumor xenograft. Starting at day 15 after tumor cell inoculation at a mean tumor volume of 30 mm^3, six weekly doses of 3, 10, and 30 µg BNT141 RNA-LNP and 800 µg IMAB362 were administered (Figure 2a, Figure S4). Treatment of mice with 30 µg BNT141 significantly inhibited tumor growth compared to controls (Luc RNA-LNP, $p = .01$; Saline, $p = .014$). The 30 µg BNT141 regimen trended toward being superior to the 800 µg IMAB362 regimen; 3 or 10 µg BNT141 RNA-LNP were less effective. The mean tumor volumes on the last day of the study (day 56), relative to the Luc RNA-LNP control cohort, were smallest for the 30 µg BNT141 RNA-LNP dose cohort (55%), followed by the cohorts that received 3 µg BNT141 (75%), 800 µg IMAB362 (78%) and 10 µg BNT141 (82%) (Figure 2b).

BNT141 repeated dosing of rodents results in sustained exposure with biologically active RiboMab01 without signs of toxicity

Next, we studied how IV administration of the RNA-LNP translates to exposure to the encoded pharmacologically active antibody in rodents. Upon IV administration of luciferase-encoding RNA-LNP in mice, we detected expression of the encoded protein to be largely confined to the liver followed by 1–2 orders of magnitudes lower signal in the spleen (Figure 2c–d). We analyzed the *in vivo* production of RiboMab01 in mice after single (study duration, 21 days) and weekly (5 doses; study duration, 42 days) injections of BNT141 RNA-LNP. Single injections (1 to 30 µg BNT141) revealed RiboMab01 maximum plasma concentrations (C_{max}, 7 to 456 µg/mL) and persistence (7 to 21 days) to be dose-dependent, but not dose-proportional (Figure S3, Table S1). These findings were largely confirmed in a single-dose PK study in Wistar rats (Figure S3B, Table S2). Weekly injections of 30 or 10 µg BNT141 maintained stable RiboMab01 expression in mice, while expression was not stable with injections of 3 or 1 µg (Figure 2e, Table S3). The 30 µg dose level led to RiboMab01 accumulation with each injection (C_{max}, 730 to 1,073 µg/mL from 1st to 5th dose). RiboMab01 plasma concentrations peaked in mice approximately 24 h after BNT141 administration for all doses. Notably, injecting mice with 3 µg (single) or 10 µg (weekly) doses of BNT141 produced peak RiboMab01 plasma levels comparable to 40 µg (single) or 80 µg (weekly) doses of IMAB362. Anti-RiboMab01 antibodies were detected in mice dosed with 1 to 10 µg BNT141 in concentrations that inversely correlated to the dose (Figure S5A).

RiboMab01 present in the serum of mice 7 days after BNT141 treatment mediated CLDN18.2-specific ADCC, depending on the administered BNT141 RNA-LNP dose, indicating full functionality of *in vivo*-produced antibody (Figure 2f).

Release of pro-inflammatory cytokines (IL-6, IFN-α, TNF-α) and chemokines (MCP-1 and MIP-1α) at moderate levels was detectable 6 h after IV administration of BNT141, was transient, dose-dependent and associated with the RNA-LNP rather than the encoded antibody (Figure S6).

No clinical signs of systemic toxicity and no BNT141 treatment-associated loss in animal body weight were observed (Figure S3C-E) for any of the tested BNT141 dosing regimens in all species in the above-described pharmacokinetic studies. Given that CLDN18.2 is a gastric epithelia lineage marker, we were specifically interested in gastric toxicity. As the above studies were not designed to assess toxicity, and with only 30 µg BNT141 being the highest dose tested, we conducted an exploratory toxicity study in mice with a specific focus on gastric toxicity. A single IV administration of 4 mg/kg (~80 µg) BNT141 did not affect stomach weight absolute or relative to body weight (data not shown) and no indications for immune-cell infiltration, inflammation, or necrosis in the gastric mucosa were observed macroscopically or upon microscopic inspection (Figure S7). Again, no clinical signs or effects on animal body weight were observed in this single dose non-GLP study.

BNT141 repeated dosing of nonhuman primates results in sustained exposure with biologically active RiboMab01

To explore pharmacokinetics in a model that is closer to human, we resorted to NHP. Three groups of cynomolgus monkeys ($n = 3$/group) were administered different doses of BNT141 (0.1, 0.4, or 1.6 mg/kg) once a week for three administrations. All three groups exhibited dose-dependent and sustainable RiboMab01 serum levels through day 21 and detectable levels until the end of study at day 35 (Figure 3a, Table S4). The three BNT141 doses of 0.1, 0.4, and 1.6 mg/kg yielded RiboMab01 C_{max} values of 3, 22, and 41 µg/mL post first injection and 5, 36, and 23 µg/mL post-third injection, respectively. T_{max} was 48 h after the first injection and 24 to 48 h after the third injection. The overall mean half-life of RiboMab01 was 82 h (intergroup range: 53 to 102 h). As observed in mice, RiboMab01 exposure was BNT141 dose-dependent but not dose-proportional. The cynomolgus monkeys dosed with 1.6 mg/kg BNT141 developed anti-RiboMab01 antibodies toward the end of the second dosing cycle (Figure S5B), while anti-RiboMab01 antibodies were detected in two monkeys in the 0.4 mg/kg BNT141 dose group at the end of the study (data not shown).
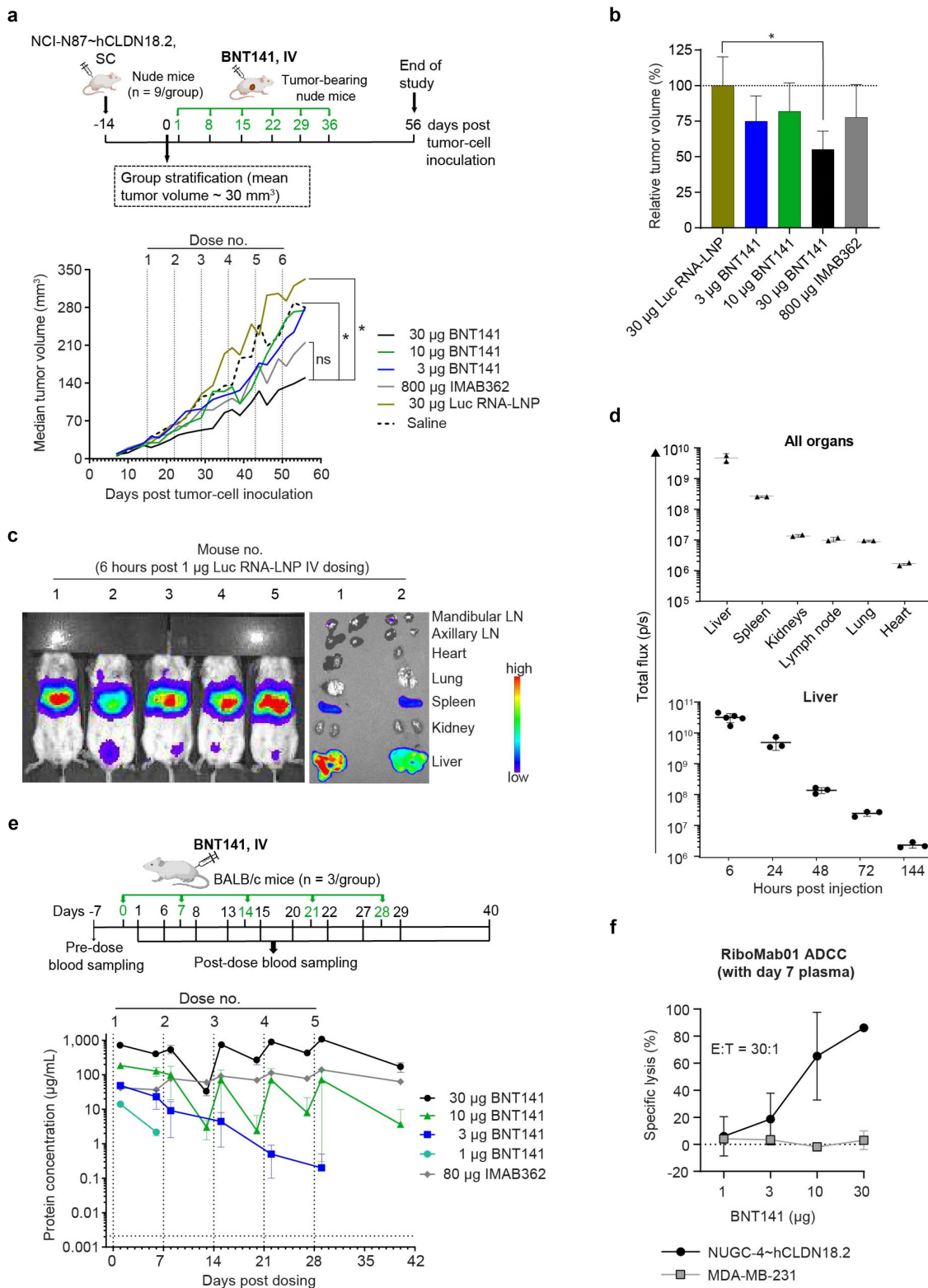
Figure 2. Weekly BNT141 administration slows tumor growth and results in stable exposure to biologically functional RiboMab01 in mice. (a) Top panel, tumor-bearing Hsd:Athymic Nude-Foxn1 nu/nu mice were treated with different doses of BNT141 or 800 μg reference IMAB362. Control animals were treated with 30 μg Luc RNA-LNP or saline. Bottom panel, Median tumor growth over time. Vertical dotted lines indicate weekly BNT141 injections. (b) Relative mean tumor volumes measured on day 56 (end of the study) and normalized to the Luc RNA-LNP group. (c) For *in vivo* imaging of RNA-LNP biodistribution, female BALB/cJRj mice received a single IV injection of Luc RNA-LNP and bioluminescence was monitored 6, 24, 48, 72, and 144 h after administration. Bioluminescence images taken 6 h after Luc RNA-LNP administration are shown for individual mice (left panel) in ventral position (*n* = 5) and single organs (right panel) of mouse #1 and mouse #2. (d) Top panel, quantification of bioluminescence in different organs 6 h after administration (*n* = 2). Bottom panel, quantification of bioluminescence in the liver (*n* = 5 for 6-h time point or *n* = 3 for all other indicated time points). Individual data points are shown along with the mean ± SD. (e) Injection schedule (top panel) and the corresponding RiboMab01 plasma concentrations (bottom panel) for female BALB/cJRj mice repeatedly dosed with BNT141 or IMAB362. Blood was sampled at the indicated time points and plasma concentrations of RiboMab01 and IMAB362 were quantified by ELISA. The horizontal dotted line represents the lower limit of quantification. (f) *Ex vivo* ADCC, mediated by RiboMab01-containing plasma from BNT141-treated mice, after 48 h of co-incubation of human PBMC with NUGC-4~hCLDN18.2 gastric adenocarcinoma cells. The Mann-Whitney U test was used for group-wise comparison (*$p < .001$). Arithmetic means ± SD are shown in E, means ± SD in F. Mouse icons adapted from BioRender. ADCC, Antibody-dependent cellular cytotoxicity; E:T, effector-to-target; Luc, Luciferase; n, number; ns, not significant; SC, subcutaneous; IV, intravenous; PBMC, peripheral blood mononuclear cells; p/s, photons per second.
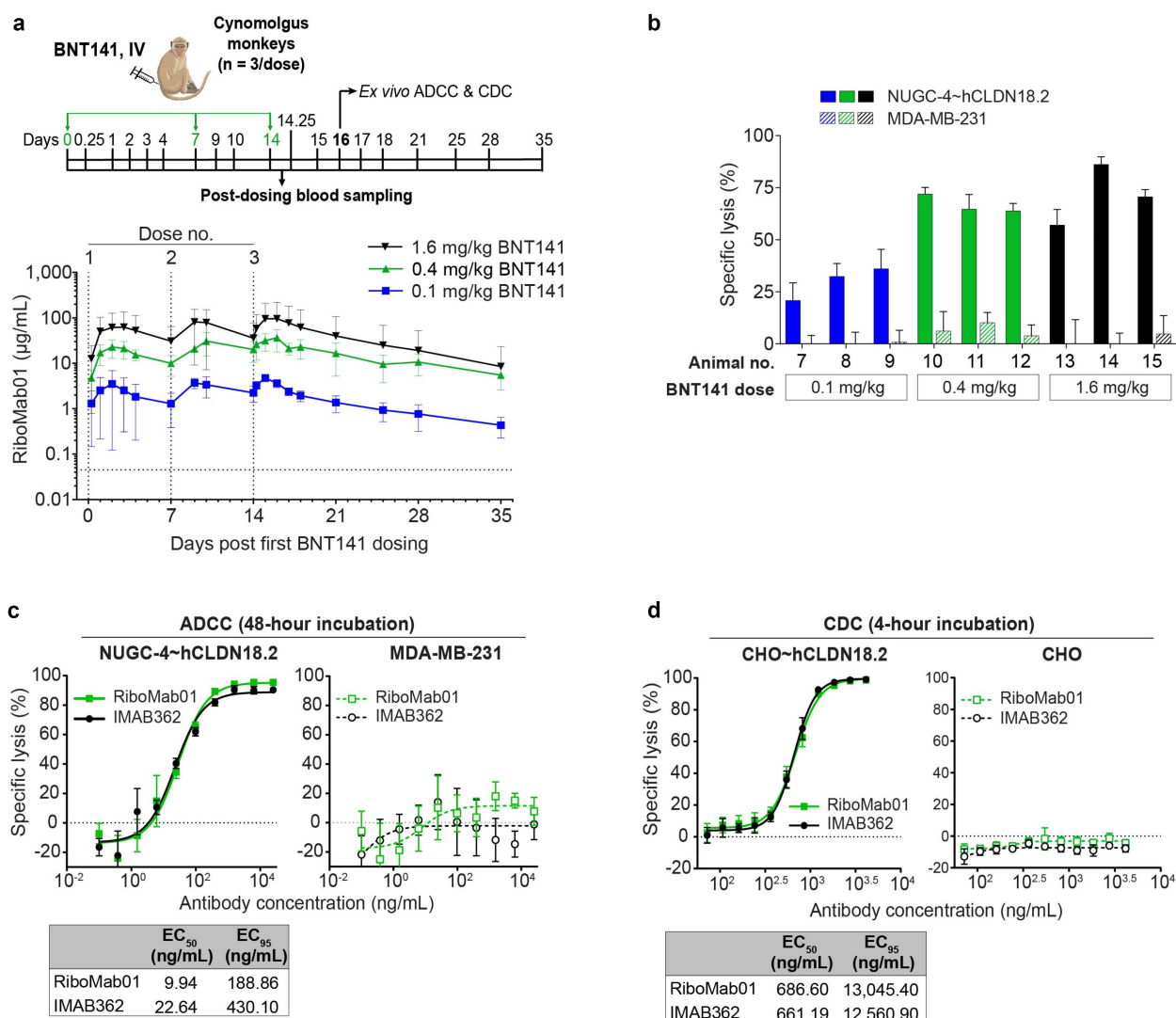
Figure 3. Repeated dosing of nonhuman primates with BNT141 results in sustained serum levels of functional RiboMab01. (a) Top panel, BNT141 was administered to female cynomolgus monkeys ($n = 3$/group) and blood was drawn at the indicated time points. Bottom panel, RiboMab01 serum concentrations upon repeated BNT141 dosing. Shown are arithmetic means ± SD. The horizontal dotted line represents the lower limit of quantification. (b) *Ex vivo* ADCC activity of RiboMab01 expressed in monkeys (serum sampled 168 h after first BNT141 dose) with NUGC-4~hCLDN18.2 target cells and human PBMC (E:T ratio of 30:1). CLDN18.2-negative MDA-MB-231 cells served as negative control. Specific lysis was measured after 48 h of incubation. (c) ADCC (48-h incubation) and (d) CDC (4-h incubation) mediated by RiboMab01 in serum collected 48 h after third dosing of animal no. 14. CDC was performed with 25% human serum as complement source. CHO~hCLDN18.2 served as target cells and wildtype CHO as negative control. IMAB362 served as reference protein. Data are mean ± SD of technical triplicates (b–d). Cynomolgus monkey icon adapted from BioRender. ADCC, Antibody-dependent cellular cytotoxicity; CDC, Complement-dependent cytotoxicity; CHO, Chinese hamster ovary; EC50, half maximal effective concentration; E:T, effector-to-target; IV, intravenous; n, number.

RiboMab01 expressed in cynomolgus monkeys and contained in their serum 7 days after the first injection mediated CLDN18.2-specific ADCC in co-cultures of human PBMC and NUGC-4~hCLDN18.2 target cells at a 30:1 E:T ratio (Figure 3b). Serum from animal no. 14 (BNT141 dose: 1.6 mg/kg) with the highest RiboMab01 C_{max} showed CLDN18.2-restricted ADCC and CDC comparable to IMAB362 (ADCC EC_{50}: 9.94 ng/mL vs. 22.64 ng/mL; CDC EC_{50}: 686.2 ng/mL vs. 661.1 ng/mL) (Figure 3c–d). Thus, the antibody encoded by IV administered RNA-LNP is also readily bioavailable and functional in larger animals.

Discussion

Our study provides preclinical characterization of BNT141, an LNP-formulated RNA that encodes for the amino acid sequence of IMAB362/Zolbetuximab, a chimeric ADCC- and CDC-mediating anti-CLDN18.2 IgG1 late-stage clinical monoclonal antibody drug candidate.[12,13,15] We show that IV administered BNT141 is expressed in the liver, the encoded protein is secreted and circulates in the vascular system. In mice, rats and cynomolgus monkeys, sustained exposure of treated animals to the antibody at concentrations above or around the antibody's EC_{50} is achieved by repeated weekly intravenous administration.

BNT141 RNA-LNP has potent anti-tumor activity in mice, mediating growth inhibition of CLDN18.2-positive tumor xenografts, while RiboMab01 recovered from BNT141 treated mice kills CLDN18.2-expressing cells *in vitro*. Of note, 30 µg BNT141 achieved comparable or better tumor control than 800 µg IMAB362, similar to

observations with RNA-encoded versions of trastuzumab (anti-HER2)[21] and pembrolizumab (anti-PD-1).[22]

We have not observed indications for potential safety signals related to the encoded antibody's mode of action. This is in line with other data: the lack of expression of CLDN18.2 in the vast majority of normal tissues in animals and humans and its assumed inaccessibility for antibodies in gastric epithelia, the only constitutively expressing cell type,[1,2,23] the absence of cross-reactivity of IMAB362 with other normal tissues in immunohistochemistry confirmed in this paper and a favorable safety profile with manageable gastric adverse events reported for IMAB362/Zolbetuximab in several clinical studies.[12,13,15] Associated with the RNA-LNP platform, we have observed transient release of pro-inflammatory cytokines at moderate levels that most likely is attributable to the lipid formulation. Of note, pro-inflammatory cytokines may even contribute to the anti-tumor activity by promoting the function of antibody-mediated immune effector mechanisms, e.g., IFN-α can support the cytotoxicity of natural killer cells,[24] which is crucial for ADCC-inducing therapeutic IgG antibodies such as RiboMab01. As innate immune stimulatory thresholds differ between the species investigated herein and humans, further understanding of these signals will have to come from the ongoing clinical trials.

PK studies in rodents and cynomolgus monkeys confirmed *in vivo* expression of biologically active RiboMab01 and comparable interspecies T_{max} values of 24 to 48 h. In mice, a RiboMab01 C_{max} of more than 1,000 µg/ml was achieved after five weekly injections of 30 µg BNT141, compared with a C_{max} of approximately 140 µg/ml obtained with 80 µg IMAB362. This is consistent with observations by other investigators that RNA-encoded antibodies had better dose-exposure ratios than their purified antibody counterparts.[21,22,25,26] Cynomolgus monkeys administered 1.6 mg/kg BNT141 showed a mean C_{max} of 23 µg/mL RiboMab01, which is approximately 115-fold higher than the *ex vivo* ADCC EC_{95} value (0.2 µg/mL), suggesting that even low doses of RNA-LNP may be sufficient to achieve biologically relevant antibody exposure in patients. Despite receiving similar doses of BNT141 relative to body weight, cynomolgus monkeys exhibited an initial C_{max} approximately 10-fold lower than observed for mice or rats, suggesting nonlinear dose extrapolation between NHPs and rodents.

In conclusion, the preclinical pharmacology of BNT141, along with existing proof-of-concept studies,[17,21,22,27] supports the exploration of antibody-encoding RNA therapeutics for cancer therapy.

Acknowledgments

Disclosure statement

All authors are current or former employees of, and own stock and/or stock options in, BioNTech SE. Ö.T. is the Chief Medical Officer of BioNTech SE and is named as an inventor on patents related to IMAB362/Zolbetuximab. U.Ş. is the Chief Executive Officer of BioNTech SE. A patent application has been submitted by BioNTech SE for BNT141. H.B-M., U.E., C.R.S., L.F., C.L., J.D., K.B., U.Ş., and Ö.T. are named as inventors on issued or pending patents related to BNT141. U.Ş. and Ö.T. have received royalties and consultancy fees from Astellas Pharma.

Funding

ORCID

Claudia Lindemann http://orcid.org/0000-0002-6987-2398
Anuhar Chaturvedi http://orcid.org/0000-0002-9597-3010
Martin Rao http://orcid.org/0000-0002-0579-1097
Uğur Şahin http://orcid.org/0000-0003-0363-1564

Data availability statement

Additional supporting data cannot be made publicly available due to a pending patent application but are available from the corresponding author upon reasonable request.

References

1. Sahin U, Koslowski M, Dhaene K, Usener D, Brandenburg G, Seitz G, Huber C, Türeci Ö. Claudin-18 splice variant 2 is a pan-cancer target suitable for therapeutic antibody development. Clin Cancer Res. 2008 Dec 1;14(23):7624–7634. doi:10.1158/1078-0432.CCR-08-1547.

2. Türeci Ö, Koslowski M, Helftenbein G, Castle J, Rohde C, Dhaene K, Seitz G, Sahin U. Claudin-18 gene structure, regulation, and expression is evolutionary conserved in mammals. Gene. 2011 Aug 1;481(2):83–92. doi:10.1016/j.gene.2011.04.007.

3. Coati I, Lotz G, Fanelli GN, Brignola S, Lanza C, Cappellesso R, Pellino A, Pucciarelli S, Spolverato G, Guzzardo V, et al. Claudin-18 expression in oesophagogastric adenocarcinomas: a tissue microarray study of 523 molecularly profiled cases. Br J Cancer. 2019 Jul;121(3):257–263. doi:10.1038/s41416-019-0508-4.

4. Karanjawala ZE, Illei PB, Ashfaq R, Infante JR, Murphy K, Pandey A, Schulick R, Winter J, Sharma R, Maitra A, et al. New markers of pancreatic cancer identified through differential gene expression analyses: claudin 18 and annexin A8. Am J Surg Pathol. 2008 Feb;32(2):188–196. doi:10.1097/PAS.0b013e31815701f3.

5. Tanaka M, Shibahara J, Fukushima N, Shinozaki A, Umeda M, Ishikawa S, Kokudo N, Fukayama M. Claudin-18 is an early-stage marker of pancreatic carcinogenesis. J Histochem Cytochem. 2011 Oct;59(10):942–952. doi:10.1369/0022155411420569.

6. Wöll S, Schlitter AM, Dhaene K, Roller M, Esposito I, Sahin U, Türeci O. Claudin 18.2 is a target for IMAB362 antibody in pancreatic neoplasms. Int J Cancer. 2014 Feb 1;134(3):731–739. doi:10.1002/ijc.28400.

7. Shinozaki A, Shibahara J, Noda N, Tanaka M, Aoki T, Kokudo N, Fukayama M. Claudin-18 in biliary neoplasms. Its significance in the classification of intrahepatic cholangiocarcinoma. Virchows Arch. 2011 Jul;459(1):73–80. doi:10.1007/s00428-011-1092-z.

8. Micke P, Mattsson JS, Edlund K, Lohr M, Jirstrom K, Berglund A, Botling J, Rahnenfuehrer J, Marincevic M, Ponten F, et al. Aberrantly activated claudin 6 and 18.2 as potential therapy targets in non-small-cell lung cancer. Int J Cancer. 2014 Nov 1;135(9):2206–2214. doi:10.1002/ijc.28857.

9. Tureci Ö, Mitnacht-Kraus R, Woll S, Yamada T, Sahin U. Characterization of zolbetuximab in pancreatic cancer models. Oncoimmunology. 2019;8(1):e1523096. doi:10.1080/2162402X.2018.1523096.

10. Lordick F, Thuss-Patience P, Bitzer M, Maurus D, Sahin U, Türeci Ö. Immunological effects and activity of multiple doses of zolbetuximab in combination with zoledronic acid and interleukin-2 in a phase 1 study in patients with advanced gastric and gastroesophageal junction cancer. J Cancer Res Clin Oncol. 2023 Jan 6;149(9):5937–5950. doi:10.1007/s00432-022-04459-3.

11. Sahin U, Schuler M, Richly H, Bauer S, Krilova A, Dechow T, Jerling M, Utsch M, Rohde C, Dhaene K, et al. A phase I dose-escalation study of IMAB362 (Zolbetuximab) in patients with advanced gastric and gastro-oesophageal junction cancer. European J Cancer. 2018 Sep;100:17–26. doi:10.1016/j.ejca.2018.05.007.

12. Türeci Ö, Sahin U, Schulze-Bergkamen H, Zvirbule Z, Lordick F, Koeberle D, Thuss-Patience P, Ettrich T, Arnold D, Bassermann F, et al. A multicentre, phase IIa study of zolbetuximab as a single agent in patients with recurrent or refractory advanced adenocarcinoma of the stomach or lower oesophagus: the MONO study. Ann Oncol. 2019 Sep 1;30(9):1487–1495. doi:10.1093/annonc/mdz199.

13. Sahin U, Tureci O, Manikhas G, Lordick F, Rusyn A, Vynnychenko I, Dudov A, Bazin I, Bondarenko I, Melichar B, et al. FAST: a randomised phase II study of zolbetuximab (IMAB362) plus EOX versus EOX alone for first-line treatment of advanced CLDN18.2-positive gastric and gastro-oesophageal adenocarcinoma. Ann Oncol. 2021 May;32(5):609–619. doi:10.1016/j.annonc.2021.02.005.

14. Lordick F, Al-Batran SE, Ganguli A, Morlock R, Sahin U, Türeci Ö. Patient-reported outcomes from the phase II FAST trial of zolbetuximab plus EOX compared to EOX alone as first-line treatment of patients with metastatic CLDN18.2+ gastroesophageal adenocarcinoma. Gastric Cancer. 2021 May;24(3):721–730. doi:10.1007/s10120-020-01153-6.

15. Shitara K, Lordick F, Bang YJ, Enzinger P, Ilson D, Shah MA, Van Cutsem E, Xu RH, Aprile G, Xu J, et al. Zolbetuximab plus mFOLFOX6 in patients with CLDN18.2-positive, HER2-negative, untreated, locally advanced unresectable or metastatic gastric or gastro-oesophageal junction adenocarcinoma (SPOTLIGHT): a multicentre, randomised, double-blind, phase 3 trial. Lancet. 2023 Apr 14;401(10389):1655–1668. doi:10.1016/S0140-6736(23)00620-7.

16. Xu R-H, Shitara K, Ajani JA, Bang Y-J, Enzinger PC, Ilson DH, Lordick F, Van Cutsem E, Gallego Plazas J, Huang J, et al. Zolbetuximab + CAPOX in 1L claudin-18.2+ (CLDN18.2 +)/HER2− locally advanced (LA) or metastatic gastric or gastro-esophageal junction (mG/GEJ) adenocarcinoma: primary phase 3 results from GLOW. J Clin Oncol. 2023;41(36_suppl):405736–405736. doi:10.1200/JCO.2023.41.36_suppl.405736.

17. Stadler CR, Bahr-Mahmud H, Celik L, Hebich B, Roth AS, Roth RP, Kariko K, Tureci O, Sahin U. Elimination of large tumors in mice by mRNA-encoded bispecific antibodies. Nat Med. 2017 Jul;23(7):815–817. doi:10.1038/nm.4356.

18. Sahin U, Türeci Ö, Brandenburg G, Usener D, inventors. Monoclonal antibodies against claudin-18 for treatment of cancer. United States patent US8425902B2. 2013.

19. Holtkamp S, Kreiter S, Selmi A, Simon P, Koslowski M, Huber C, Tureci O, Sahin U. Modification of antigen-encoding RNA increases stability, translational efficacy, and T-cell stimulatory capacity of dendritic cells. Blood. 2006 Dec 15;108 (13):4009–4017. doi:10.1182/blood-2006-04-015024.

20. Orlandini von Niessen AG, Poleganov MA, Rechner C, Plaschke A, Kranz LM, Fesser S, Diken M, Lower M, Vallazza B, Beissert T, et al. Improving mRNA-based therapeutic gene delivery by expression-augmenting 3' UTRs identified by cellular library screening. Mol Ther. 2019 Apr 10;27(4):824–836. doi:10.1016/j.ymthe.2018.12.011.

21. Rybakova Y, Kowalski PS, Huang Y, Gonzalez JT, Heartlein MW, DeRosa F, Delcassian D, Anderson DG. mRNA delivery for therapeutic anti-HER2 antibody expression in vivo. Mol Ther. 2019 Aug 7;27(8):1415–1423. doi:10.1016/j.ymthe.2019.05.012.

22. Wu L, Wang W, Tian J, Qi C, Cai Z, Yan W, Xuan S, Shang A. Intravenous delivery of RNA encoding anti-PD-1 human monoclonal antibody for treating intestinal cancer. J Cancer. 2022;13 (2):579–588. doi:10.7150/jca.63991.

23. Hashimoto I, Oshima T. Claudins and gastric cancer: an overview. Cancers. 2022;14(2):290. doi:10.3390/cancers14020290.

24. Kwaa Abena KR, Talana CAG, Blankson JN, Silvestri G. Interferon alpha enhances NK cell function and the Suppressive capacity of HIV-Specific CD8+ T cells. J Virol. 2019;93(3):10.1128/jvi.01541–18. doi:10.1128/jvi.01541-18.

25. Kose N, Fox JM, Sapparapu G, Bombardi R, Tennekoon RN, de Silva AD, Elbashir SM, Theisen MA, Humphris-Narayanan E, Ciaramella G, et al. A lipid-encapsulated mRNA encoding a potently neutralizing human monoclonal antibody protects against chikungunya infection. Sci Immunol. 2019 May 17;4(35): eaaw6647. doi:10.1126/sciimmunol.aaw6647.

26. Pardi N, Secreto AJ, Shan X, Debonera F, Glover J, Yi Y, Muramatsu H, Ni H, Mui BL, Tam YK, et al. Administration of nucleoside-modified mRNA encoding broadly neutralizing antibody protects humanized mice from HIV-1 challenge. Nat Commun. 2017 Mar 2;8(1):14630. doi:10.1038/ncomms14630.

27. Thran M, Mukherjee J, Ponisch M, Fiedler K, Thess A, Mui BL, Hope MJ, Tam YK, Horscroft N, Heidenreich R, et al. Schlake T. mRNA mediates passive vaccination against infectious agents, toxins, and tumors. EMBO Mol Med. 2017 Oct;9(10):1434–1447. doi:10.15252/emmm.201707678.